Cureus

Fluorescence-Guided Tumor Visualization Using the Tumor Paint BLZ-100

David S. Kittle [1], Adam Mamelak Cedars-Sinai Medical Center [2], Julia E. Parrish-Novak [3], Stacey Hansen [4], Rameshwar Patil [5], Pallavi R. Gangalum [5], Julia Ljubimova [5], Keith L. Black [1], Pramod Butte [1]

1. Neurosurgery, Cedars-Sinai Medical Center 2. Neurosurgery, Cedars-Sinai Medical Center , Los Angeles, USA 3. Research, Blaze Bioscience 4. Other, Blaze Bioscience 5. Department of Neurosurgery, Cedars-Sinai Medical Center

✉ **Corresponding author:** David S. Kittle, davidscott.kittle@cshs.org
Disclosures can be found in Additional Information at the end of the article

Abstract

Objective: Intraoperatively delineating between normal tissue and tumorous tissue in real time ensures near-complete tumor resection. Recently, this has been shown by using targeted fluorescent agents that bind to tumor cells, conjugated to a fluorophore that can be detected with fluorescence imaging methods. One promising tumor ligand for in vivo fluorescence imaging is chlorotoxin (CTX), which has been conjugated to indocyanine green (ICG), and named BLZ-100. In conjunction with BLZ-100, we are nearing completion of developing and optimizing an imaging system (SIRIS) for in-vivo imaging of BLZ-100 for use in surgical resections of gliomas.

Methods: BLZ-100 concentrations were prepared in a 5% intralipid solution. The concentrations tested ranged from 1 μMolar to 100 picoMolar. Serial dilutions of ICG were prepared in aqueous concentrations ranging from 3.23 mM to 66.1 pM. The tray was imaged using the commercial Zeiss Pentero surgical microscope and SIRIS. Finally, BLZ-100 was injected in animals implanted with intracranial human glioblastoma cells 48 hours prior to euthanasia. Fluorescence imaging was performed by SIRIS, a camera system developed that simultaneously acquires both white light and NIR images, while combining these images via super-imposition on a high-definition (HD) video monitor.

Results: The NIR imaging system developed (SIRIS) is capable of visualizing concentrations of ICG down to 1 nM and BLZ-100 to well below 1 nM (extinction at 100 pM). Glioma and medulloblastoma implanted in mouse brains demonstrated that BLZ-100 has a high affinity for both tumor types compared to normal brain where there is no measurable fluorescence.

Conclusions: We have developed a camera system for NIR detection of fluorescence tumor ligands, and demonstrated the utility of this camera for detecting BLZ-100 both in vivo and in vitro. The system is designed to permit simultaneous tumor resection and NIR visualization, and has been developed as an ergonomic and surgeon-friendly device.

Categories: Neurosurgery, Oncology
Keywords: intraoperative fluorescence, tumor resection, blz-100, infrared imaging, fluorescence image-guided surgery, fluorescence, tumor visualization, icg, glioma

Introduction

The current 18-month survival rate of patients with glioblastoma treated with complete surgical resection ranges from 15% to 34%, making glioma one of the most lethal tumors [1], with a mean survival of 14 months. Gliomas have a reported incidence of 10 per 100,000 per year and result in 13,000 deaths per year, accounting for more person-years of life lost than any other tumor [2]. Although there are multiple treatment options available, such as chemotherapy or radiation therapy, surgical resection remains a primary treatment [3-5]. The role of extent of resection in prolonging patient survival is controversial [2, 6-7]; however, there is substantial evidence that minimizing tumor residual will decrease the likelihood of recurrence [8-9]. Many publications over the previous decades have demonstrated that extent of resection is the single most important determinant of outcome for patients with high-grade gliomas, and the single most important predictor of survival [10-12]. Evidence also suggests that a more complete surgical resection of gliomas correlates with a higher progression-free interval and may prolong life expectancy [2, 6-7].

One of the primary challenges in surgical removal of brain tumors is the identification and differentiation of tumor tissue from normal brain. This problem is exacerbated by the infiltrative nature of gliomas. In order to overcome these challenges, surgeons have employed various imaging techniques, including image-guided surgery based on preoperative MRI (magnetic resonance imaging) scans, intra-operative MRI (iMRI), and intra-operative ultrasound. There are several other newer techniques, which have demonstrated potential, including time resolved fluorescence spectroscopy [13-18] and Raman spectroscopy [19-22], but these techniques are very hard to deploy in the operating conditions and require complicated hardware.

Tumor-specific ligands for fluorescence-guided resection of brain tumors

Targeted fluorescent agents rely upon a tumor-specific ligand to bind the tumor cells, conjugated to a fluorophore that can be detected with fluorescence imaging methods. Targeted contrast agents remain the most promising path in fluorescence techniques due to their high specificity and sensitivity. Many such potential targeting agents have been reported for cancer cells [23-25].

Chlorotoxin (CTX):

One promising tumor ligand for in vivo fluorescence imaging is chlorotoxin (CTX). Chlorotoxin is a 36 amino acid peptide initially isolated from the venom of the scorpion Leiurus quinquestriatus. CTX avidly binds to malignant tumors while demonstrating only trace binding with normal human tissues [26]. Recent data has shown that CTX binds to annexin A2 receptors expressed on the membranes of malignant tumors and is then internalized. Annexin A2 receptors are expressed only internally in non-cancerous cells, while malignant cells express these receptors on the cell membrane. Clinical trials of 131I-CTX have been carried out in patients with recurrent gliomas [26-27]. In Phase I trials, intra-cavitary injection of 10-30 mCi iodine and 0.2 mg CTX resulted in prolonged local binding of CTX to the tumor cavity, with no appreciable binding elsewhere in the body. A Phase II trial demonstrated improved survival in patients receiving six intra-cavitary injections of 30 mCi 131I-CTX, and intravenous injection studies demonstrated that 131I-CTX will selectively bind to metastatic (i.e. non-glial) tumors and gliomas, and could be detected on whole body SPECT scans. All clinical trials to date conducted with CTX indicate that it has negligible toxicity in humans and can be repeatedly given without development of an antibody response. These unique properties, along with its small size and lack of immunogenicity, make CTX attractive as a ligand for targeted cancer therapies.

Fluorescent Tumor Paint:

In light of its exquisite tumor affinity, CTX was conjugated to the fluorophore Cy5.5 for in vivo fluorescence detection of tumors. In close parallel to observations from human trials with 131I-CTX, CTX:Cy5.5 avidly bound gliomas and other tumors in animal models, with subsequent identification of tumors when exposed to near infrared light (Figure *1*). In this setting, CTX:Cy5.5 was proposed as a "Tumor Paint" to ensure maximal tumor detection while avoiding injury to normal tissues. This approach is especially appealing in gliomas, as it is the infiltrating nature of the tumor that typically limits "margin free" resections. Furthermore, a CTX-based Tumor Paint can also be used in other malignancies, such as breast, head, neck, colon, melanoma, and lung cancers, to ensure complete resection and the identification of micrometastases. Hence, the development of a viable tumor-specific and non-toxic Tumor Paint can have widespread clinical ramifications.
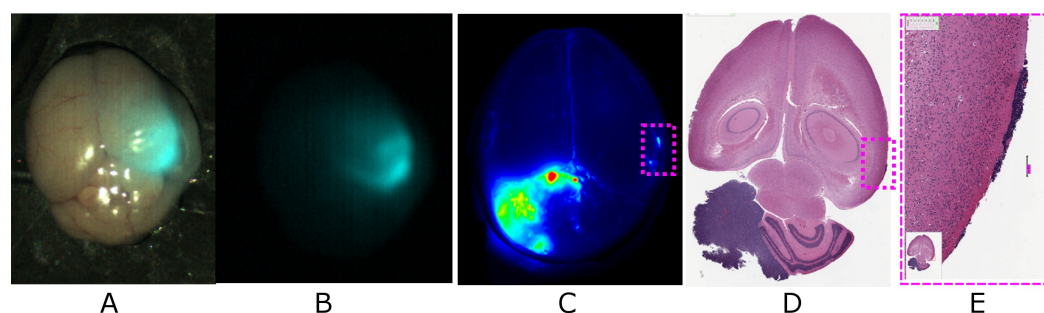

FIGURE 1: ICG fluorescence

A-B) Injection of BLZ-100 and imaged with our SIRIS. C-E) Intravenous BLZ-100 administered to mice with spontaneous medulloblastoma, imaged with a commercial fluorescence imager.

Near–Infrared Imaging:

Over the past several years, intraoperative imaging using invisible near infrared (NIR) fluorescence has gained interest as the preferred method for intraoperative fluorescence-guided surgery. Whereas visible light penetrates tissue on the micrometer scale, NIR light (700–900 nm) can travel millimeters-and up to centimeters-through blood and tissue. This increased photon transport improves the identification of targets below the surface. As biological tissue exhibits almost no auto-fluorescence in the NIR spectrum, the signal-to-background contrast can be maximized using fluorescent contrast agents responsive to NIR light. NIR imaging does not use ionizing radiation, only a Class 1m excitation laser source, making it an inherently safe technique for clinical use. Furthermore, NIR light is invisible to the human eye (NIR fluorescent targets are visible only on the display monitor) and does not alter the appearance of the surgical field. Unique to this system is the capability of filtering out the NIR excitation, while allowing white light and NIR fluorescence to pass through to the detector with greater than 90% efficiency.

BLZ-100 Tumor Paint^{TM}:

In light of the promising results obtained from studies of CTX:Cy5.5, indocyanine green (ICG), a near infrared dye that is FDA approved for human use as a vascular contrast dye, was conjugated to CTX. ICG has low toxicity in animals (LD$_{50}$ 50-80 mg/kg) and is approved for use in humans at doses up to 2 mg/kg. ICG has been used clinically for decades in vascular imaging and surgeries, and more recently in perfusion studies and sentinel lymph node mapping.

Chlorotoxin, a 36 amino acid, 4 kDa peptide (reviewed in [27, 29-30]) that contains four disulfide bonds, forms a compact three-dimensional structure. BLZ-100 is a covalently bound CTX:ICG molecule. BLZ-100 has many functional features that make it well-suited for clinical use. Near infrared light has far greater tissue penetration than ultraviolet light and a narrow emission spectrum, permitting filter optimization for fluorescence detection. There is little absorption by hemoglobin in these wavelengths, so intervening normal tissue does not attenuate the signal to the same extent seen with fluorescent imaging agents in other wavelengths [31]. Finally, there is very low tissue auto-fluorescence at the emission wavelength, enabling very good signal to noise and sharp definition of tumor boundaries.

We are nearing completion of developing and optimizing an imaging system for in-vivo imaging of BLZ-100 for use in surgical resections of gliomas. In this paper, we present the results of our imaging system when used to detect BLZ-100 in-vitro as well as our preliminary results in mice implanted with brain tumors.

Materials And Methods

Fluorescence imaging system

To address the need of a clinically relevant tool for NIR fluorescence-guided resection of tumors, we developed a camera system that simultaneously acquires both white light and NIR images, combining these images via super-imposition on a high-definition (HD) video monitor. The clinical prototype system (SIRIS) consists of a high-definition camera that is sensitive in both the visible and NIR wavelengths (CMOSIS CMV2000, 2/3", 2040X1086, 340fps, Camera Link interface) (Figure 2).
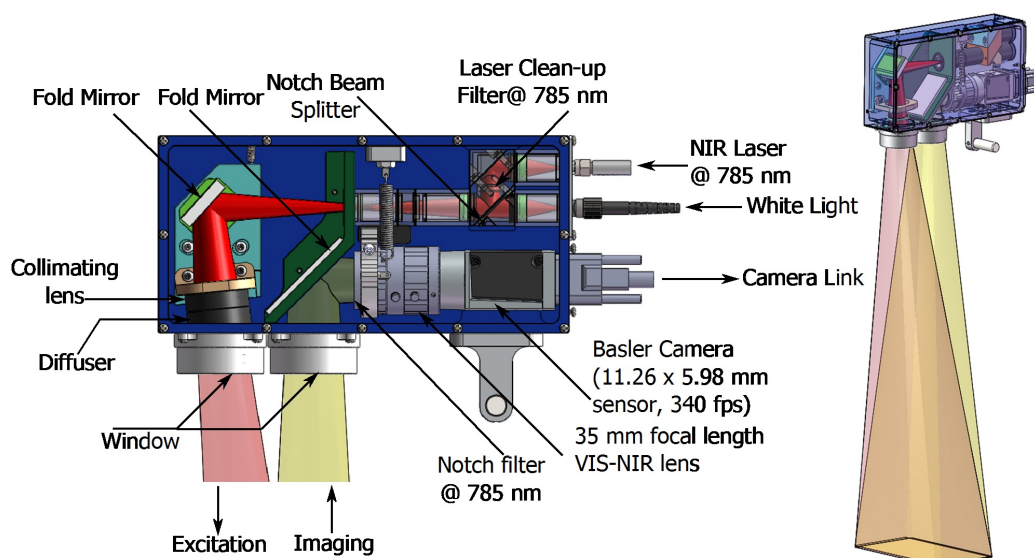

FIGURE 2: SIRIS clinical prototype

The SIRIS unit measures 7.75" x 3.74" x 2.06" and weighs approximately 3.8 lbs, allowing it to be attached to commercial endoscope holders. With a focal distance of 45 cm, it sits far outside the surgical field. The camera output is connected to an image processing computer and then fed to a HD video monitor for display.

A fixed focal length lens (35 mm VIS-NIR Compact Fixed Focal Length Lens, Edmund Optics) was attached using a C-mount. A 785 nm notch filter to filter out the excitation light from the return image (Semrock, 785 nm StopLine® single-notch filter, NF03-785E-25) was attached in front of the objective lens. NIR excitation is provided via a 785 nm laser diode (Coherent, Model

FAP800-12W-777.0, Santa Clara, CA, USA), while white light is provided through the use of four LEDs (blue, cyan, green, and red), each independently controlled for optimal white balance. Both the NIR and white light sources are combined in a single unit (Lumencor ASTRA light engine, Beaverton, OR) and remotely controlled via RS-232. The laser diode requires a clean-up filter to reduce the side lobe wavelengths of the laser. The spectrums of the filters and laser are shown in Figure 3. The camera acquires both white light and NIR fluorescence images via a camera link interface to a frame grabber (BitFlow, KBN-PCE-CL4-SP) to a computer. The NIR images are given a false color and added to the white light image. Processing is done using a graphics processing unit (GPU) due to the high data rate (718 Mbytes/sec) and real-time requirements. The resultant HD quality images, superimposed with fluorescent maps of BLZ-100 distribution, can be used to direct intraoperative detection and resection of tumors. The camera system can detect BLZ-100 in nanomolar to picomolar concentrations. Since the images are collected digitally, the detection sensitivity can be adjusted utilizing analog and digital gain and thresholded to maximize detection in the NIR range, as well as providing artificial color maps.
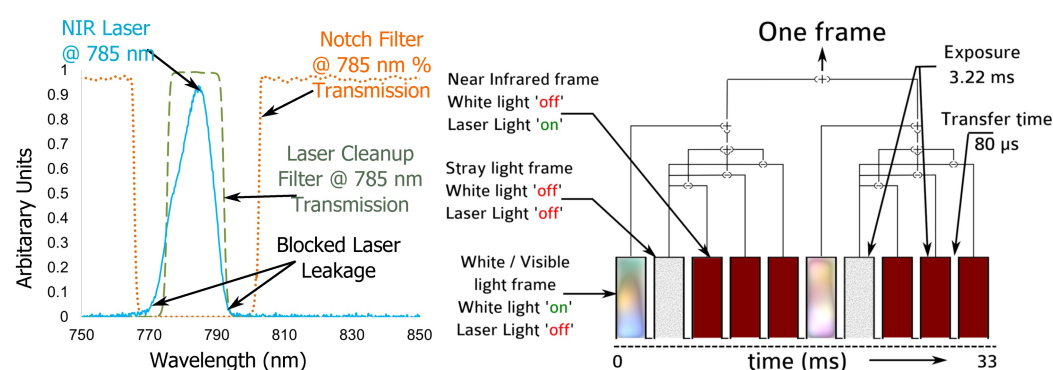

FIGURE 3: SIRIS system operation and wavelength

(Left) Wavelengths filtered through the SIRIS system, showing the spectrum of the excitation laser, laser cleanup filter following fiber input of the camera, and blocked spectral range allowed back into the camera by the notch filter at the objective lens. (Right) Pulsing of excitation: 10 frames are captured in one 'frame' sequence that will be displayed to the viewer. The subframes are captured at 300 fps and video display at 30 fps.

The NIR and visible frames are captured using a single detector by reading out a series of five frames shown in Figure 3. First, a stray light frame is captured to subtract the ambient light from the next three NIR frames, illuminated by strobing the NIR laser. The fifth frame is then captured by strobing the white light source. The three NIR frames are then added together and demosaiced. The white light image is demosaiced and finally added to the false-colored NIR frame and displayed. At 340 frames per second (fps), the five frame sequence is repeated every 14.7 ms for a display rate of 68 fps. For additional sensitivity, the next five fames can be processed and added to the previous frame to double the NIR integration time (total of 17.4ms), while reducing the displayed frame rate to 34 fps. The visible frame will not show any latency due to only the last frame being used. The NIR frames will have some artifacts due to subtraction and addition over a finite period of time. The advantage to using multiple short frames is immunity to high ambient lighting conditions causing saturation of a single longer-integration NIR fluorescence frame. Other advantages include the use of multiple exposures at differing integration times for HDR composites. The operating field and fluorescence images yields a high dynamic range that is challenging to capture with conventional methods of imaging.

SIRIS was custom engineered and built (Optical Support, Inc, Tucson, AZ) for integration into

common surgical systems, such as the Storz articulating arm (Figure 4). Two 1 mm optical fibers attach to the camera housing to transmit the 785 nm laser and white light, sourced from the Lumencor light engine. Two Camera Link cables for high-speed data transmission attach to the Basler acA2000-340kc area scan CMOS sensor. The system is designed to be draped during surgical procedures for sterile environments.
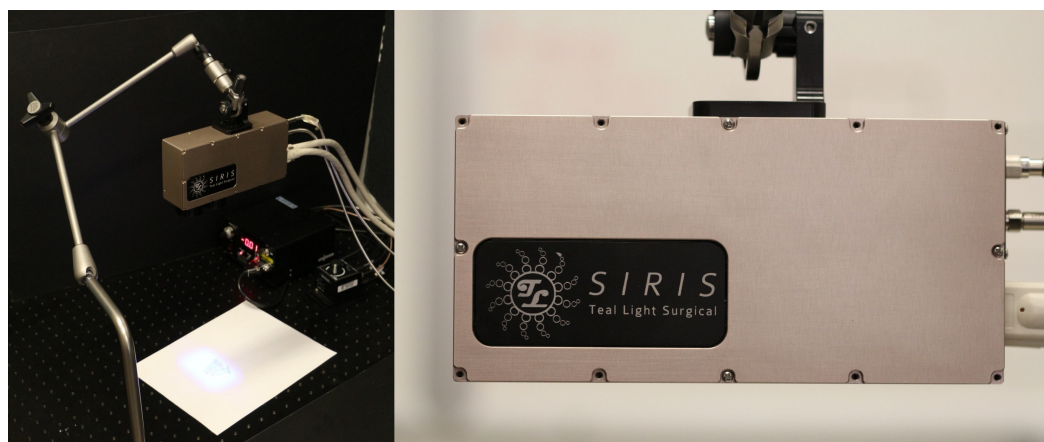

FIGURE 4: SIRIS clinical prototype instrument

The clinical prototype SIRIS attached to the Storz endoscope articulating arm. The illumination profile of the system is rectangular to match the HD resolution of the camera and typical displays used in the operating room. Two fibers and two camera link cables attach to the back of the system, while a surgical drape coves the system for entering into the sterile field.

Laser safety compliance

Particular concern was attributed to the safety of the 785 nm laser excitation. The diode laser is capable of up to 6W of output at the fiber port of the Lumencor device. Class IV laser restrictions are debilitating in the surgical field, so a combination of diffusers and reduced output were used to lower the actual output at the SIRIS to a Class 1M laser device. This enables the use of the camera without any safety training or goggles. The laser flux at the surgical site was optimized to maintain high fluorescence, while minimizing danger due to eye injury.

Imaging resolution

The spatial resolution of the SIRIS camera was measured by diffuse illumination of a 1951 USAF resolution target at a thee degree angle, directly measuring a slanted edge for calculating the line spread function. The Fourier transform of this is then proportional to the spatial frequency response, shown as a modulation transfer function in Figure 5. This method measures the optical performance of the camera system, while reducing the undersampling of the CMOS sensor pixels. With optimal focus of the objective lens set for white light, an 11 micron feature (45 cycles per mm) can be resolved with 40% contrast for the visible frame and 0.2% contrast for the NIR frame. If the NIR frame is optimally focused, it nearly resembles the contrast of the white light frame. The discrepancy in the spatial resolution is due to chromatic focal shift of the objective lens. The achromatic design enables perfect focus at two wavelengths with defocus forming a quadratic through these zero points. The NIR spectrum lies along the asymptote of the quadratic, causing the focus to shift rapidly as the wavelength increases. The design requirement for the SIRIS system required 500 micron feature detection at 20% contrast for a 350 mm working distance in both NIR and visible wavelengths. Additional measurements of the USAF target for 500 micron features (Group 0, Element 1 on the USAF target) at the 350 mm object distance show a contrast of 92.5% for white light and 55% for NIR. The decision of spatial resolution and sensitivity will have to be determined for all such systems requiring small

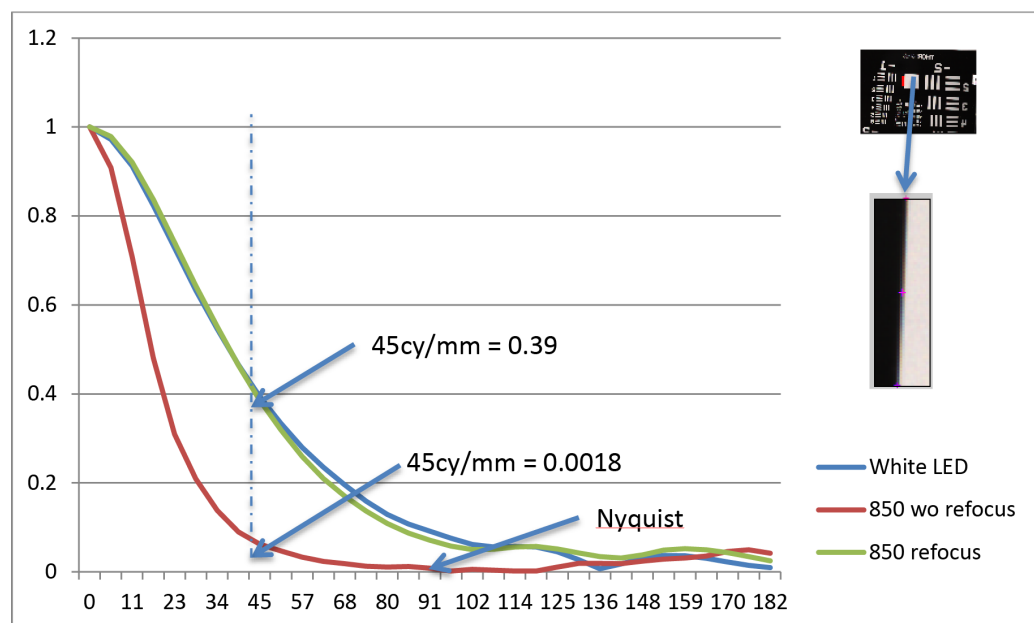optical volume and large spectral bandwidths.

FIGURE 5: SIRIS imaging resolution

Modulation transfer function of the SIRIS, measured at the maximum aperture of f/1.6. The chromatic focal shift is evident in the 850 nm curve when the objective lens has not been refocused to this wavelength. Stopping down the objective lens to f/4 or higher significantly reduces this aberration, while increasing the required exposure time to maintain similar sensitivity.

Intracranial tumors in animals

BLZ-100 was also tested in animals implanted with intracranial human glioblastoma cells. Animals were treated according to the approved Cedars-Sinai Medical Center Institutional Animal Care and Use Committee protocols (Protocol #2420). Athymic mice (NCr-nu/nu homozygous) were obtained from NCI. 5×10^5 human glioblastoma cells (LN229) were stereotactically implanted into the right basal ganglia of mice under ketamine and dexmedetomidine intraperitoneal anesthesia [32]. The animals were closely monitored and used for the experiment after about six weeks post inoculation, when the tumors had reached maximum size.

The tumor-bearing mice were intravenously injected via tail vein once using a 30-gauge needle on a 1 ml syringe, at a rate of 50 µl over three seconds under isoflurane anesthesia. Three mice received 20 nmol of BLZ-100, while a second cohort of three mice received 20 nmol ICG. A third set of mice received PBS as control. Following drug administration, the mice were observed for several hours for any physical symptoms or behavioral changes. Forty-eight hours after injection, animals were anesthetized via intraperitoneal injection of combination ketamine and dexmedetomidine, and euthanized via cervical dislocation.

The mice were then placed securely in a stereotactic head frame, and a craniectomy was performed over the right half of the brain. In situ tumor imaging was performed with our SIRIS prototype to determine if the tumor could be visualized, after which the brain and other organs were removed for individual imaging and processing.

Cureus

Results

Intralipid study

In order to test the sensitivity of BLZ-100 detection at varying concentrations, BLZ-100 concentrations were prepared in a 5% intralipid solution. The concentrations tested were: 1 µMolar, 100 nanoMolar, 10 nanoMolar, 1 nanoMolar, and 100 picoMolar. The fluorescence intensity at an integration time of 40 ms and analog camera gain of 140 are shown in Figure 6. 1µM and 0.1µM concentrations are both saturated on the detector, while the 10 nM concentration show an intensity of 75 and the 100 pM a signal of only one count higher than background.
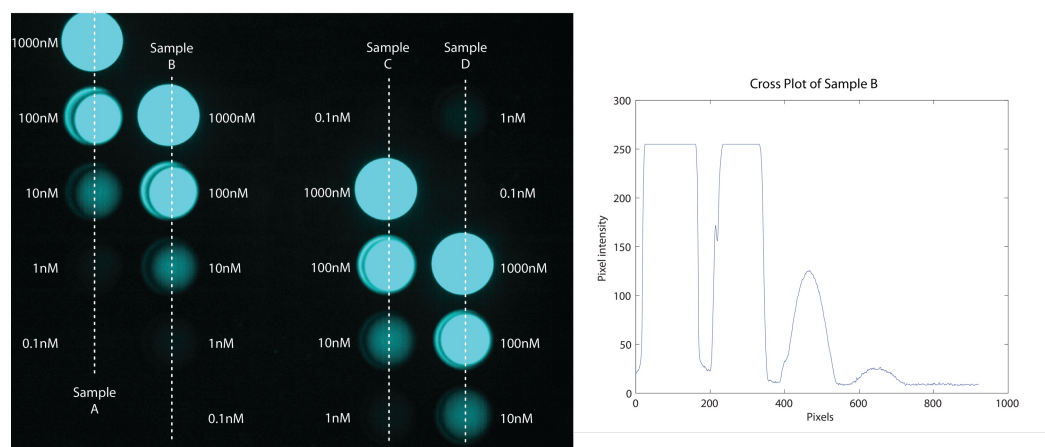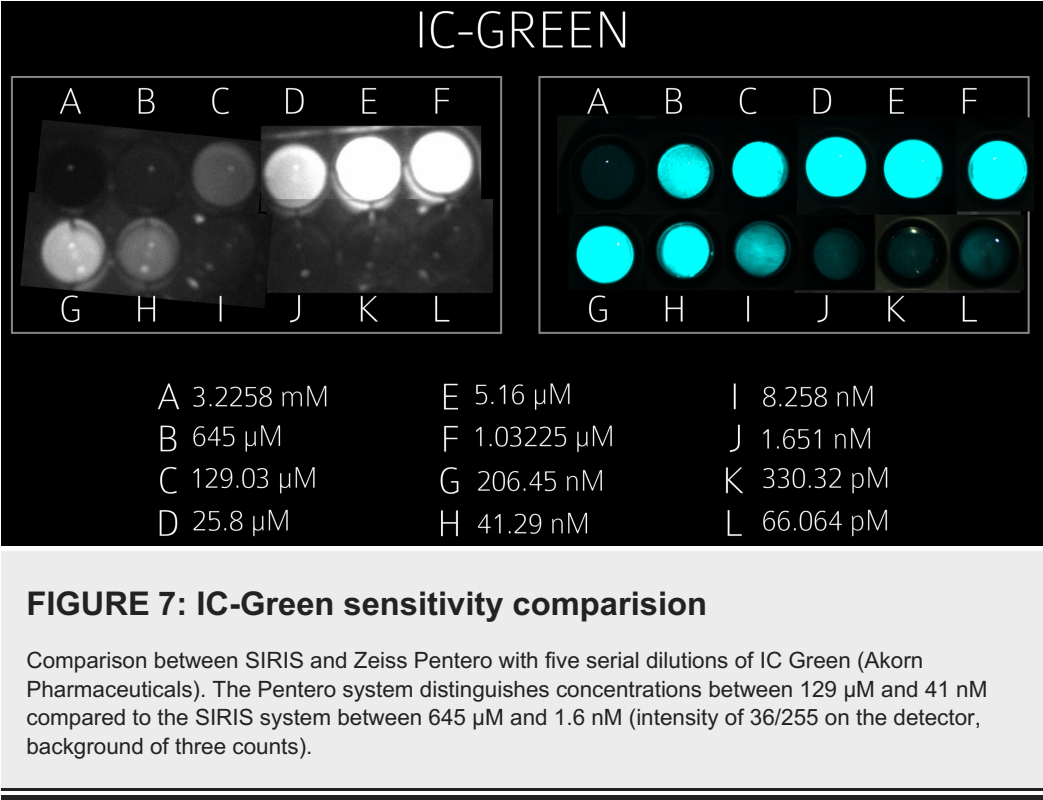

FIGURE 6: Sensitivity for BLZ-100 in intralipid

(Left) NIR image (no white light) showing fluorescence intensity of five different concentrations of BLZ-100 in 5% intralipid. Camera integration time was 40 ms total and relatively low analog gain of 140 (in range of 33-512). (Right) Cross-plot of intensity image. The 1 nanoMolar concentration is weak and the 100 picoMolar concentration is near extinction.

ICG comparison study

Serial dilutions of ICG were prepared with the following aqueous concentrations: 3.23 mM, 645 µM, 129 µM, 25.8 µM, 5.16 µM, 1.03 µM, 206 nM, 41.3 nM, 8.26 nM, 1.65 nM, 330 pM, and 66.1 pM. The tray was imaged using Zeiss Pentero surgical microscope and the SIRIS camera, both in NIR imaging mode. The Pentero recovers concentrations down to 41 nM, whereas the SIRIS system recovers concentrations between 1 - 8 nanoMolar. Also, higher concentrations are visible in the SIRIS system, where even 645 µM is visible compared to 129 µM in the Pentero.

FIGURE 7: IC-Green sensitivity comparision

Comparison between SIRIS and Zeiss Pentero with five serial dilutions of IC Green (Akorn Pharmaceuticals). The Pentero system distinguishes concentrations between 129 µM and 41 nM compared to the SIRIS system between 645 µM and 1.6 nM (intensity of 36/255 on the detector, background of three counts).

Photobleaching

Photobleaching of BLZ-100 was observed when in solution with intralipid. After 70 minutes of infusion with the laser, a decay of 75% from the original intensity was observed. However, when attached to tissue, there was no photobleaching after one hour of continuous imaging. The mean intensity was initially at 106 counts, and after one hour, increased to 108 due to the tissue drying and increased concentration of BLZ-100 in the tissue.

In vivo study (brain)

Mice injected with BLZ -100 and sacrificed after 48 hours showed significant fluorescence from the tumorous tissues, while there was no fluorescence observed from the mice injected with ICG. BLZ-100 seemed to accumulate in the glioma. Additionally, fluorescence from BLZ-100 was able to show a deeper metastasis. The organs harvested from the mice were also recorded for fluorescence (Figure 8). There was no visible fluorescence from stomach, heart, and lung. Kidney and liver showed detectable amounts of BLZ-100.
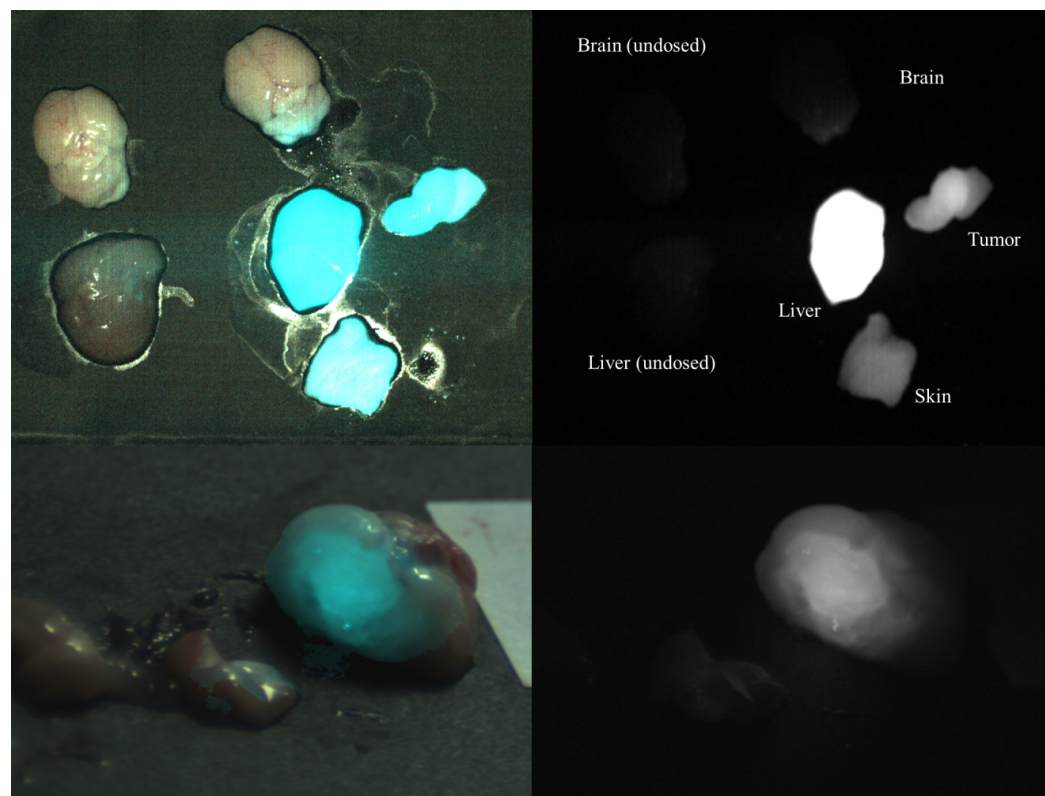
FIGURE 8: BLZ-100 fluorescence in various tissues

Various tissues imaged through the SIRIS system. The left column includes visible and NIR fluorescence overlaid, the right column shows the NIR without visible light. The top two panels show a control mouse brain without BLZ-injected and liver, skin, and tumor of an injected mouse. The bottom two panels show a glioma in the brain of a mouse after injection of BLZ-100.

Medulloblastoma

BLZ-100 injected into a mouse with medulloblastoma showed significant fluorescence. Comparisons were made between SIRIS and the commercial Odyssey CLx Infrared Imaging System (LI-COR, Lincoln, NE). SIRIS showed comparable sensitivity, while saturating in the high-concentration areas. The Odyssey had higher dynamic range and did not saturate. Methods are currently being implemented to increase the dynamic range of SIRIS by utilizing multiple NIR frames.
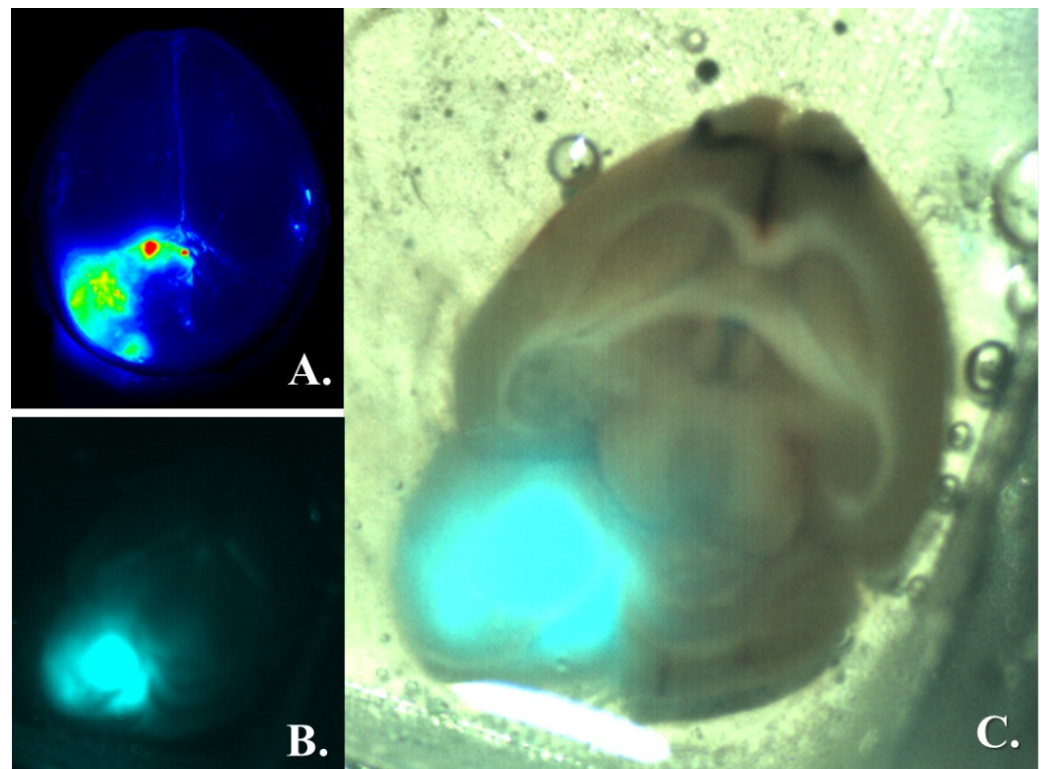
FIGURE 9: BLZ-100 fluorescence in medulloblastoma

BLZ-100 fluorescence in a mouse medulloblastoma. A) Odyssey system, B) SIRIS NIR only, C) SIRIS Visible + NIR.

Animal study (canine)

Collaboration is currently underway with the VCA West Los Angeles Animal Hospital (VCA protocol #2013-003) where we have provided SIRIS for fluorescent imaging of BLZ-100 injected canines during surgical procedures. This clinical site has proved to provide valuable insight into surgical applications of SIRIS, sensitivity, and operating room requirements, and surgeon feedback while using SIRIS.

FIGURE 10: SIRIS in the operating room

Use of SIRIS during a veterinary surgery. The SIRIS camera can be seen directly above the operating table.

Video data from SIRIS

Video from a phantom surgery is shown in Video 1. A phantom was prepared by combining gelatin, 20% Intralipid (Baxter, Deerfield, IL), indocyanine green (IC-Green, Akorn), and water.

VIDEO 1: Model tumor with ICG implanted in gelatin

View video here: http://youtu.be/fObSKF4xlgQ

A second phantom was prepared using 500 ml water, 5 ml Intralipid, and 31.3 grams of gelatin. ICG stock was prepared at 1 mM concentration and diluted to 200 nM by placing in 10 mL of gelatin solution and injected into the 500 mL gelatin solution. The lesion with ICG is shown in Video 2. Note a slight visibility on the surface before incision and very bright visibility after cutting though the gelatin solution.
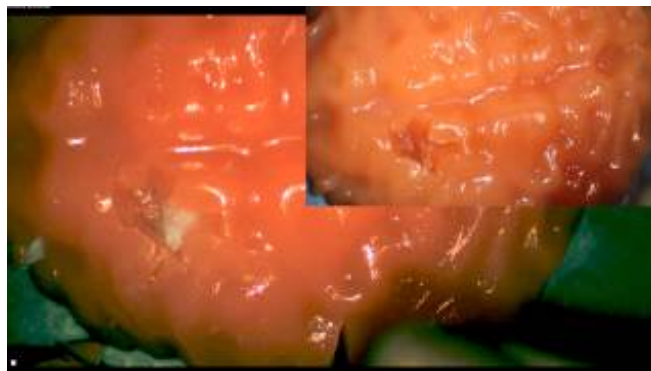
VIDEO 2: Modeled brain tumor in a brain phantom made of Gelatin

View video here: http://youtu.be/BvAMv4GZMTM

A third video shows real-time intraoperative fluorescence of a canine lymphoma during a surgical procedure and ex-vivo imaging. The uptake of BLZ-100 was poor for this surgery, so the concentrations of BLZ-100 in the lymphoma are very low, likely less than 500 pM. However, the tumor is still quite visible at the extremely low concentration at video-rate imaging.
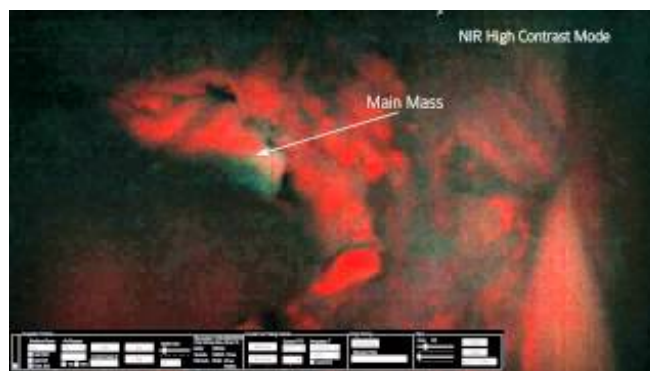
VIDEO 3: Canine lymphoma surgery using SIRIS

View video here: http://youtu.be/fYE45GuuURo

Discussion

To address the need of a clinically relevant tool for NIR fluorescence-guided resection of tumors, we developed a camera system that simultaneously acquires both white light and NIR images, and combines these images via super-imposition on a high-definition (HD) video monitor. The "proof of concept" system (SIRIS) acquires both white light and NIR fluorescence images. These are captured via a camera link interface to a computer. The NIR images are displayed by false coloring and added to the white light image. The resultant HD quality images superimposed with fluorescent maps of BLZ-100 distribution can be used to direct intraoperative detection and resection of tumor. The camera system can detect BLZ-100 in picomolar concentrations. Since the images are collected digitally, the detection sensitivity can be adjusted utilizing software gain and threshold to maximize detection in the NIR as well as providing artificial color maps. Our current prototype version incorporates the excitation and visible light, allowing it to be utilized in a clinical setting that demands an entirely integrated unit. SIRIS can be draped for a sterile field and will tolerate the rigorous demands of the operating room. The ultimate goal of this research is to build a device which will be designed to attach to a commercially available exoscope (VITOM-90®, Storz), although the system can also be configured to work with an endoscope or a standard operating microscope (OM).

Synergy between imaging device and imaging agent

A major aspect of the innovative approach employed is that the fluorescent imaging agent, the detection device utilized for fluorescence, and white light illumination device used during surgical resection have all been developed simultaneously. Typically, an imaging agent is developed by a lab or company with little attention paid to the device that will be used clinically to image it. In turn, clinical trials are performed with the use of commercially available imaging devices that are not designed to optimize fluorescence detection of the molecule, or are not easy to use in a clinical setting. Conversely, commercially available imaging systems that are available for intraoperative use are not optimized to the specific fluorophore being utilized, but are rather designed to be broad and inclusive, or to facilitate use of already available and FDA approved imaging agents, such as ICG or fluorescein. Our approach overcomes this hurdle by integrating both the device and the fluorescent agent into a single platform, designed specifically to reflect realistic use in the operating room environment. SIRIS has been designed with these parameters in mind, and the close synergistic relationship between our institution and the manufacturer of BLZ-100 will help to ensure these goals are met.

From our current experiments, we can see that our imaging system is able to detect BLZ-100 down to 1 nM of concentration with strong contrast. The safe level of laser fluence for

excitation without the use of protective goggles is considered to be around 25 mW/cm^2. With protective goggles, it is possible to increase the fluence to at least twice the amount of energy, which will allow us to detect even lower concentrations of BLZ-100. The mice that were injected with BLZ-100 showed significant accumulation of BLZ-100 in glioma, while being completely absent in normal tissue. Additionally, due to high penetration of NIR wavelengths, it was possible to detect a metastatic lesion that would have been missed due to its distance from the main mass (Figure 7). Although these are preliminary results, they point at the benefit of using BLZ-100 for real-time tumor diagnosis. There was no fluorescence from the glioma in mice injected with only ICG, suggesting the fluorescence in the BLZ-100 injected mouse brain is due to binding of CTX to the glioma cells. BLZ-100 is cleared in the liver and is excreted by the kidneys, which can be seen by presence of fluorescence in both kidney and liver. All the other organs were negative for presence of BLZ-100.

Near infrared imaging and other tumor ligands

Recently, NIR technology has been utilized to detect fluorescent tumor ligands. These cancer-targeted molecules can be used to specifically isolate tumors for resection. Huang, et al. recently reported on the utility of an integrin receptor, integrin $\alpha_v\beta_3$, as a target for an NIR fluorescent probe in a mouse model [33]. They found it to be a practical, affordable, simple, and time-efficient method to localize glioma tissue and aid resection. A fluorophore conjugated to a peptide that specifically binds the glioblastoma integrin was utilized as the ligand. Sexton, et al. showed that smaller ligands have the potential to better bind to the infiltrative edges of the tumor [34]. This was demonstrated by the use of a fluorescently labeled affibody, which had more clear differentiation of the brain-tumor interface than the significantly larger full antibody to the same receptor. Most recently, a novel type 2 cannabinoid receptor (CB$_2$R)-targeted probe that is highly expressed in invasive cancer has been tested as another fluorescent probe [35], with many more in development. Even if BLZ-100 fails to work in clinical settings, our SIRIS system is ideally suited to be utilized with all other NIR targeted fluorescent probes, and can easily be optimized for any specific wavelength as needed. As such, we are hopeful this represents a clinically viable platform for all NIR agents for fluorescence-guided resection of gliomas.

Other studies investigating fluorescence-guided resection: 5-ALA and fluorescein

Multiple prospective studies and randomized controlled trials investigating fluorescence have been reported in the literature (Table 1). A prospective series on 52 patients published in 2000 showed that ALA-guided FGR was sensitive, specific, and resulted in gross total resection in 63% of patients [36]. Another similar prospective study on 114 consecutive intracranial lesions found a sensitivity between 83-87% and a complete resection rate of 77% [37].

Study Type	Authors	Number of patients	Flourophore	Tumor type	Main Outcomes
Prospective	Stummer, et al., 2000 [36]	52	ALA	Gliomas	Sens: 99.6%, Spec: 81.6%, CRR: 63%
Prospective	Hefti, et al., 2008 [7]	74	ALA	Gliomas, other	"Solid": Sen. 98%, Spec. 100%, CRR: NR "Vague": 76%, 85%, NR
Prospective	Eljamel, et al., 2009 [37]	114	ALA	Gliomas, pituitary tumors, metastases	Sen. 83-87%, Spec. NR, CRR: 77%
RCT, multicenter	Stummer, et al., 2006 (ALA-Study group) [38]	279 (131 in control group)	ALA	Glioma	GTR in 65% (vs. 35%); 6 months PFS: 41.0% (vs. 21.1%).
RCT	Eljamel, et al., 2008 [6]	27 (14 in control group)	ALA + Photofrin, PDT	GBM	MS: 52.8 weeks (vs. 24.6); PFS: 8.6 (vs. 4.8 months); 20 pts. higher KPS; CRR: 77%
Prospective	Koc, et al., 2008 [39]	82 (33 in control group)	Fluorescein	GBM	GTR of 83 vs. 55%; no statistically significant difference in survival
Prospective	Shinoda, et al., 2003 [40]	32	Fluorescein	GBM	GTR in 84.4%; no statistically significant difference in survival
Prospective	Kuroiwa, et al., 1998 [41]	10	Fluorescein	Glioma	GTR in 80%

TABLE 1: Summary of previous published reports on ALA use in brain tumors.

The ALA-study group reported their findings of a randomized controlled trial (RCT) and found those with ALA-enhanced resection had a 19.9% higher progression-free survival (PFS) with an associated 29% higher rate of complete tumor resection. Another RCT reported in 2008 utilizing ALA and Photofrin, along with photodynamic therapy for GBM, reported similar positive outcomes on complete resection and PFS [6]. Despite these positive outcomes, no study to date has shown an increase in overall survival with the use of FGR. Nonetheless, these encouraging data with an ultraviolet agent suggest that results with NIR FGR should be even more promising and useful.

Conclusions

We have developed a camera system for NIR detection of fluorescence tumor ligands and demonstrated the utility of this camera for detecting BLZ-100 both in vivo and in vitro. The system is designed to permit simultaneous tumor resection and NIR visualization, and has been developed as an ergonomic and surgeon-friendly device.

References

1. Brandes AA, Tosoni A, Franceschi E, Reni M, Gatta G, Vecht C: Glioblastoma in adults. Crit Rev Oncol Hematol. 2008, 67:139-52. 10.1016/j.critrevonc.2008.02.005
2. Eljamel MS: Fluorescence image-guided surgery of brain tumors: Explained step-by-step . Photodiagnosis Photodyn Ther. 2008, 5:260-3. 10.1016/j.pdpdt.2008.11.003
3. Ducray F, Dutertre G, Ricard D, Gontier E, Idbaih A, Massard C: Advances in adults' gliomas biology, imaging and treatment (article in French). Bull Cancer. 2010, 97:17-36. 10.1684/bdc.2009.1019
4. Fazekas JT: Treatment of grades I and II brain astrocytomas. The role of radiotherapy . Int J Radiat Oncol Biol Phys. 1977, 2:661-6.
5. Robins HI, Lassman AB, Khuntia D: Therapeutic advances in malignant glioma: current status and future prospects. Neuroimaging Clin N Am. 2009, 19:647-56. 10.1016/j.nic.2009.08.015
6. Eljamel MS, Goodman C, Moseley H: ALA and Photofrin fluorescence-guided resection and repetitive PDT in glioblastoma multiforme: a single centre Phase III randomised controlled trial. Lasers Med Sci. 2008, 23:361-7.
7. Hefti M, von Campe G, Moschopulos M, Siegner A, Looser H, Landolt H: 5-aminolevulinic acid induced protoporphyrin IX fluorescence in high-grade glioma surgery: a one-year experience at a single institutuion. Swiss Med Wkly. 2008, 138:180-5. 2008/11/smw-12077
8. Behbahaninia M, Martirosyan NL, Georges J, Udovich JA, Kalani MY, Feuerstein BG, Nakaji P, Spetzler RF, Preul MC: Intraoperative fluorescent imaging of intracranial tumors: A review . Clin Neurol Neurosurg. 2013, 115:517-28. 10.1016/j.clineuro.2013.02.019
9. Stummer W, Reulen HJ, Meinel T, Pichlmeier U, Schumacher W, Tonn JC, Rohde V, Oppel F, Turowski B, Woiciechowsky C, Franz K, Pietsch T; ALA-Glioma Study Group: Extent of resection and survival in glioblastoma multiforme: identification of and adjustment for bias. Neurosurg. 2008, 62:564-76. 10.1227/01.neu.0000317304.31579.17
10. Berger MS: Malignant astrocytomas: Surgical aspects. Semin Oncol. 1994, 21:172-85.
11. Byar DP, Green SB, Strike TA: Prognostic Factors for Malignant Glioma. Oncology of the Nervous System. Walker MD (ed): Springer US, 1983. Vol. 12:379-395. 10.1007/978-1-4613-3858-1_14
12. Sanai N, Berger MS: Glioma extent of resection and its impact on patient outcome . Neurosurg. 2008, 62:753-64. 10.1227/01.neu.0000318159.21731.cf
13. Ardeshirpour Y, Chernomordik V, Zielinski R, Capala J, Griffiths G, Vasalatiy O, Smirnov AV, Knutson JR, Lyakhov I, Achilefu S, Gandjbakhche A, Hassan M: In vivo fluorescence lifetime imaging monitors binding of specific probes to cancer biomarkers. PLoS One. 2012, 7:e31881. 10.1371/journal.pone.0031881

14. Butte PV, Fang Q, Jo JA, Yong WH, Pikul BK, Black KL, Marcu L: Intraoperative delineation of primary brain tumors using time-resolved fluorescence spectroscopy. J Biomed Opt. 2010, 15:027008. 10.1117/1.3374049

15. Butte PV, Mamelak AN, Nuno M, Bannykh SI, Black KL, Marcu L: Fluorescence lifetime spectroscopy for guided therapy of brain tumors. Neuroimage. 2011, 54:S125-35. 10.1016/j.neuroimage.2010.11.001

16. Marcu L: Fluorescence lifetime techniques in medical applications. Ann Biomed Eng. 2012, 40:304-31. 10.1007/s10439-011-0495-y

17. Masilamani V, Das BB, Secor J, AlSalhi M, Devanesan S, Prasad S, Rabah D, Alfano RR: Optical biopsy of benign and malignant tissue by time resolved spectroscopy. Technol Cancer Res Treat. 2013, 12:559-63. 10.7785/tcrt.2012.500345

18. Meier JD, Xie H, Sun Y, Sun Y, Hatami N, Poirier B, Marcu L, Farwell DG: Time-resolved laser-induced fluorescence spectroscopy as a diagnostic instrument in head and neck carcinoma. Otolaryngol Head Neck Surg. 2010, 142:838-44. 10.1016/j.otohns.2010.02.005

19. Uckermann O, Galli R, Tamosaityte S, Leipnitz E, Geiger KD, Schackert G, Koch E, Steiner G, Kirsch M: Label-free delineation of brain tumors by coherent anti-stokes Raman scattering microscopy in an orthotopic mouse model and human glioblastoma. PLoS One. 2014, 9:e107115. 10.1371/journal.pone.0107115

20. Kalkanis SN, Kast RE, Rosenblum ML, Mikkelsen T, Yurgelevic SM, Nelson KM, Raghunathan A, Poisson LM, Auner GW: Raman spectroscopy to distinguish grey matter, necrosis, and glioblastoma multiforme in frozen tissue sections. J Neurooncol. 2014, 116:477-85. 10.1007/s11060-013-1326-9

21. Aguiar RP1, Silveira L Jr, Falcão ET, Pacheco MT, Zângaro RA, Pasqualucci CA: Discriminating neoplastic and normal brain tissues in vitro through Raman spectroscopy: A principal components analysis classification model. Photomed Laser Surg. 2013, 31:595-604. 10.1089/pho.2012.3460

22. Auner AW, Kast RE, Rabah R, Poulik JM, Klein MD: Conclusions and data analysis: a 6-year study of Raman spectroscopy of solid tumors at a major pediatric institute. Pediatr Surg Int. 2013, 29:129-40. 10.1007/s00383-012-3211-6

23. Bogdanov AA Jr, Lin CP, Kang HW: Optical imaging of the adoptive transfer of human endothelial cells in mice using anti-human CD31 monoclonal antibody. Pharm Res. 2007, 24:1186-92.

24. Kelly K, Alencar H, Funovics M, Mahmood U, Weissleder R: Detection of invasive colon cancer using a novel, targeted, library-derived fluorescent peptide. Cancer Res. 2004, 64:6247-51.

25. Weissleder R, Nahrendorf M, Pittet MJ: Imaging macrophages with nanoparticles. Nat Mater. 2014, 13:125-38. 10.1038/nmat3780

26. The MICAD Research Team: 131I-Chlorotoxin. Molecular Imaging and Contrast Agent Database (MICAD). 2004, http://www.ncbi.nlm.nih.gov/books/NBK23317/.

27. Mamelak AN, Jacoby DB: Targeted delivery of antitumoral therapy to glioma and other malignancies with synthetic chlorotoxin (TM-601). Expert Opin Drug Deliv. 2007, 4:175-86.

28. Veiseh M, Gabikian P, Bahrami SB, Veiseh O, Zhang M, Hackman RC, Ravanpay AC, Stroud MR, Kusuma Y, Hansen SJ, Kwok D, Munoz NM, Sze RW, Grady WM, Greenberg NM, Ellenbogen RG, Olson JM: Tumor paint: A chlorotoxin:Cy5.5 bioconjugate for intraoperative visualization of cancer foci. Cancer Res. 2007, 67:6882-8.

29. Stroud MR, Hansen SJ, Olson JM: In vivo bio-imaging using chlorotoxin-based conjugates. Curr Pharm Des. 2011, 17:4362-71.

30. Wu XS, Jian XC, Yin B, He ZJ: Development of the research on the application of chlorotoxin in imaging diagnostics and targeted therapies for tumors. Chin J Cancer. 2010, 29:626-30.

31. Thurber GM, Figueiredo JL, Weissleder R: Detection limits of intraoperative near infrared imaging for tumor resection. J Surg Oncol. 2010, 102:758-64. 10.1002/jso.21735

32. Fujita M, Lee BS, Khazenzon NM, Penichet ML, Wawrowsky KA, Patil R, Ding H, Holler E, Black KL, Ljubimova JY: Brain tumor tandem targeting using a combination of monoclonal antibodies attached to biopoly(beta-L-malic acid). J Control Release. 2007, 122:356-63.

33. Huang R, Vider J, Kovar JL, Olive DM, Mellinghoff IK, Mayer-Kuckuk P, Kircher MF, Blasberg RG: Integrin αvβ3-targeted IRDye 800CW near-infrared imaging of glioblastoma. Clin Cancer Res. 2012, 18:5731-40. 10.1158/1078-0432.CCR-12-0374

34. Sexton K, Tichauer K, Samkoe KS, Gunn J, Hoopes PJ, Pogue BW: Fluorescent affibody peptide penetration in glioma margin is superior to full antibody. PLoS One. 2013, 8:e60390.

10.1371/journal.pone.0060390

35. Zhang S, Shao P, Bai M: In vivo type 2 cannabinoid receptor-targeted tumor optical imaging using a near infrared fluorescent probe. Bioconjug Chem. 2013, 24:1907-16. 10.1021/bc400328m

36. Stummer W, Novotny A, Stepp H, Goetz C, Bise K, Reulen HJ: Fluorescence-guided resection of glioblastoma multiforme by using 5-aminolevulinic acid-induced porphyrins: a prospective study in 52 consecutive patients. J Neurosurg. 2000, 93:1003-13.

37. Eljamel MS: Which intracranial lesions would be suitable for 5-aminolevulenic acid-induced fluorescence-guided identification, localization, or resection? A prospective study of 114 consecutive intracranial lesions. Clin Neurosurg. 2009, 56:93-7.

38. Stummer W, Pichlmeier U, Meinel T, Wiestler OD, Zanella F, Reulen HJ; ALA-Glioma Study Group: Fluorescence-guided surgery with 5-aminolevulinic acid for resection of malignant glioma: a randomised controlled multicentre phase III trial. Lancet Oncol. 2006, 7:392-401.

39. Koc K, Anik I, Cabuk B, Ceylan S: Fluorescein sodium-guided surgery in glioblastoma multiforme: A prospective evaluation. Br J Neurosurg. 2008, 22:99-103. 10.1080/02688690701765524

40. Shinoda J, Yano H, Yoshimura S, Okumura A, Kaku Y, Iwama T, Sakai N: Fluorescence-guided resection of glioblastoma multiforme by using high-dose fluorescein sodium. Technical note. J Neurosurg. 2003, 99:597-603.

41. Kuroiwa T, Kajimoto Y, Ohta T: Development of a fluorescein operative microscope for use during malignant glioma surgery: A technical note and preliminary report. Surg Neurol. 1998, 50:41-8.